

Voltammetric Studies of the Metal-Ligand Interaction in Low-valent Metal-Olefin π -Complexes. II. Palladium(0) and Platinum(0) Complexes with Olefin-Diimine Mixed Ligands

Naoyuki ITO, Tetsuo SAJI,* and Shigeru AOYAGUI

Department of Chemical Engineering, Tokyo Institute of Technology, Ohokayama, Meguro-ku, Tokyo 152

(Received February 4, 1985)

Cyclic voltammograms for the reduction of Pd^0 and Pt^0 complexes with mixed ligands of diimine and olefin exhibit, respectively, two or four reversible one-electron steps. The half-wave potentials of each step give a straight line with a slope of 1.0, when plotted against the half-wave potentials of diimine ligands, and a slope smaller than 0.2, when plotted against the half-wave potentials of olefinic ligands. The half-wave potentials of the complexes are affected only a little by the difference in the central metal. These findings lead to the conclusion that each LUMO of these complexes is dominated by the diimine π^* -orbital, though it is higher-lying than the olefinic π^* -orbital in free ligands.

The changes in the molecular structure and electronic state that olefinic compounds may suffer when they are coordinated to transition metals may be worthy of note in connection with their reactions catalyzed by these metals. Usually, the former change can be detected by X-ray diffraction and the latter by absorption spectroscopy. Besides these, the specific contribution of voltammetry to the latter purpose is promising because it provides information on the ionization potential and the electron affinity, *viz.* the HOMO and LUMO energies, in contrast to absorption spectroscopy which provides information on the intramolecular relative energy levels. Knowledge of the HOMO and LUMO energies will make it possible to determine the behaviour of the frontier electron which has a dominant effect on the chemical reactivity.

Voltammetric and IR studies of $[\text{M}(\text{O})_2(\text{dibenzylideneacetone})_3]$ ($\text{M}=\text{Pd}$ and Pt ; dibenzylideneacetone = 1,5-diphenyl-1,4-pentadien-3-one) in Part I of this series have led to the conclusion that each LUMO of these complexes is twofold degenerate and delocalized over a π -framework composed of a metal and three phenyl-substituted olefinic moieties.¹⁾ This paper deals with the voltammetry of mixed ligand complexes, $[\text{M}(\text{O})\text{LoLc}]$ ($\text{M}=\text{Pd}$ and Pt ; $\text{Lo}=\text{olefinic ligand}$; $\text{Lc}=\text{diimine ligand}$), with a hope that we can discuss the change of LUMO of Lo caused by coordination.

Experimental

Ethenetetra carbonitrile (tcne), (*E*)-2-butenedinitrile (fn), dimethyl fumarate (dmf), dimethyl maleate (dmm), diethyl fumarate (def), 1,10-phenanthroline (phen) and 2,2'-bipyridine (bpy) were supplied by Tokyo Chemical Industries, maleic anhydride (ma) by Wako Pure Chemical Industries and 4,7-diphenyl-1,10-phenanthroline (d ϕ phen) by Kanto Chemical Industries. 4,4'-Dimethyl-2,2'-bipyridine (4-dmbpy), 5,5'-dimethyl-2,2'-bipyridine (5-dmbpy), and 4,4',5,5'-tetramethyl-2,2'-bipyridine (tmbpy) were gifts of Dr. Y. Ohsawa who prepared them by the literature method.²⁾

$[\text{Pd}(\text{O})\text{Lo}(\text{bpy})]$ ($\text{Lo}=\text{ma}$, dmf, and dmm) were prepared by methods found in the literature,³⁾ and other palladium complexes by similar methods. Platinum complexes were prepared by the same methods as the corresponding pal-

ladium complexes, except that the reaction mixtures were slightly heated until their colors turned yellow. The complexes were characterized by elemental analyses on C, H, and N.

The half-wave potential was identified with the midpoint of the cathodic peak potential (E_{pc}) and the anodic one (E_{pa}) of a cyclic voltammogram. The reversibilities of redox steps were judged on the basis of the separation (ΔE_p) between the E_{pc} and the E_{pa} and the ratio of the anodic peak current to the cathodic one. The base solution was 0.2 M ($1\text{M}=1\text{ mol dm}^{-3}$) tetrabutylammonium perchlorate (TBAP) in ethylene glycol dimethyl ether (DMeE). Neutral alumina (ICN W200) was added to the test solutions except for tcne, ma, and d ϕ phen, which are strongly adsorbed on alumina. Voltammetric measurements were carried out at $-30\pm 2^\circ\text{C}$ with a scan rate of 0.1 V s^{-1} , unless otherwise noted. Other experimental procedures have been previously described.⁴⁾ IR spectra were recorded with KBr plates on a Hitachi 295 IR spectrometer operated at 25°C .

Results and Discussion

The $\nu(\text{C-N})$ frequencies for $[\text{Pd}(\text{O})\text{LoLc}]$ with $\text{Lo}=\text{tcne}$ and fn , and $\text{Lc}=\text{bpy}$ and d ϕ phen, and $[\text{Pt}(\text{O})\text{Lo}(\text{d}\phi\text{phen})]$ with $\text{Lo}=\text{tcne}$ and fn fall within $2100\text{--}2240\text{ cm}^{-1}$, as those of other complexes of similar structure generally do.^{5,6)} They are lower than the $\nu(\text{C-N})$

TABLE 1. HALF-WAVE POTENTIALS FOR THE REDUCTION OF FREE LIGANDS ($E_{1/2,\text{L}}^{\text{red}}$) IN 0.2 M TBAP-DMeE AT -30°C , SCAN RATE 0.1 V s^{-1}

Ligand	$-E_{1/2,\text{L}}^{0/2-}/\text{V}^{\text{a}}$	$-E_{1/2,\text{L}}^{2-/2-}/\text{V}^{\text{a}}$
tcne	0.358	1.433 ^b
ma	1.580 ^b	—
fn	2.028 ^b	—
dmf	2.033	—
def	2.062	—
dmm	2.450 ^b	—
d ϕ phen	2.526	2.923 ^b
phen	2.667	3.264 ^b
bpy	2.766	3.368
4-dmbpy	2.823	3.388
5-dmbpy	2.899	3.504
tmbpy	2.963	3.558 ^b

a) $\pm 5\text{ mV}$ vs. $\text{Ag}/\text{AgNO}_3(\text{sat.})$. b) Cathodic peak potential.

frequencies of free olefin ligands, *i.e.* 2262 cm⁻¹ for tcne and 2246 cm⁻¹ for fn. The same lowering has been reported concerning the $\nu(\text{C}=\text{O})$ frequencies of [Pd(0)LoLc] with Lo=dmm and dmf, and Lc=bpy and phen.³ These findings may be evidence for the metal-to-olefin charge transfer and/or the back-donating bond operating in these complexes.

Cyclic voltammograms for the reduction of free ligands (L) exhibited, respectively, one or two one-

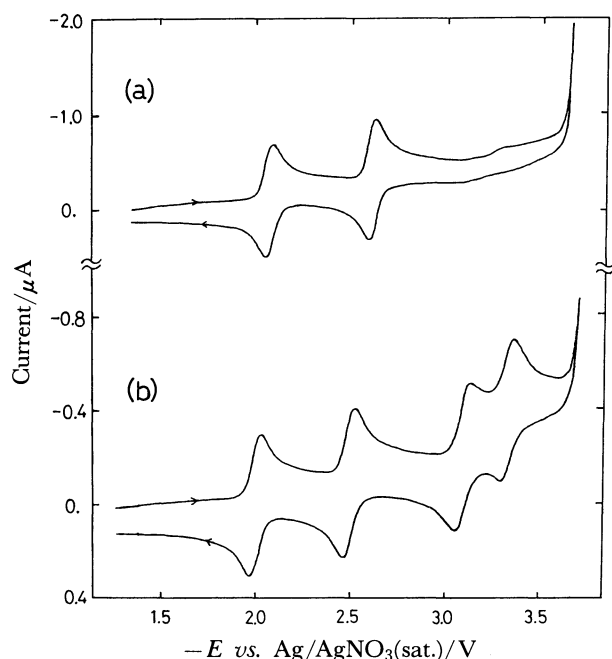


Fig. 1. Cyclic voltammograms for 0.3 mM of (a) [Pd(fn)(bpy)] and (b) [Pd(fn)(dφphen)] in 0.2 M TBAP-DMeE at -30°C, scan rate 0.1 V s⁻¹.

electron steps judged on the basis of ΔE_p . Some of these steps were reversible and others irreversible, in the sense that they had no current peaks in reversal scans. Table 1 lists the reversible half-wave potentials of L^{0/-} ($E_{1/2,L}^{0/-}$) and L^{-2/-} ($E_{1/2,L}^{-2/-}$). For irreversible steps, E_{pc} values are shown instead of $E_{1/2,L}$ values. All of the ligands studied gave no oxidation steps within the available potential range.

Cyclic voltammograms for the reduction of complexes (C) gave four one-electron steps for complexes with dφphen as Lc. Otherwise, two are given as shown in Fig. 1. The reversible steps may be tentatively assigned to C^{0/-}, C^{-2/-}, C^{-2-/3-}, and C^{-3-/4-}. No oxidation steps were observed. Table 2 summarizes the voltammetric results on complexes.

The characteristic features of Tables 1 and 2 are follows:

- (1) Each $E_{1/2,C}^{0/-}$ is by 0.4–0.9 V more positive than the corresponding $E_{1/2,L}^{0/-}$ of Lc ($E_{1/2,Lc}^{0/-}$), and by 0.1–1.5 V more negative than the $E_{1/2,L}$ of Lo ($E_{1/2,Lo}^{0/-}$).
- (2) The $E_{1/2,C}^{0/-}$ and $E_{1/2,C}^{-2/-}$ for the Pt complexes are by 0.1 V more positive than the corresponding Pd complexes.
- (3) The $E_{1/2,C}^{-2-/3-}$ and $E_{1/2,C}^{-3-/4-}$ of dφphen complexes are independent of type of metal.
- (4) The $E_{1/2,C}^{0/-} - E_{1/2,C}^{-2/-}$ values are nearly identical with the $E_{1/2,Lc}^{0/-} - E_{1/2,Lc}^{-2/-}$ values, which suggests that the coordinated Lc in a C²⁻ should be of the form Lc²⁻.⁷⁾

Figure 2 shows $E_{1/2,C}^{\text{red}}$ vs. $E_{1/2,L}^{0/-}$ plots for [M(0)-(dmf)Lc] (M=Pd and Pt) with Lc=tmbpy, 5-dmbpy, 4-dmbpy, and bpy. The straight lines were drawn in accordance with the following equation:⁸⁾

$$E_{1/2,C} = E_{1/2,L} + \text{const.}, \quad (1)$$

TABLE 2. HALF-WAVE POTENTIALS FOR THE REDUCTION OF [M(0)LoLc] ($E_{1/2,C}^{\text{red}}$) IN 0.2 M TBAP-DMeE AT -30°C, SCAN RATE 0.1 V s⁻¹

M	Lo	Lc	$-E_{1/2,C}^{0/-}/V^a$	$-E_{1/2,C}^{-2/-}/V^a$	$-E_{1/2,C}^{-2-/3-}/V^a$	$-E_{1/2,C}^{-3-/4-}/V^a$
Pd	tcne	dφphen	1.776	2.089 ^b	—	—
Pd	ma	dφphen	1.989	2.505	3.077	3.309
Pd	fn	dφphen	2.006	2.501	3.091	3.328
Pd	dmf	dφphen	2.052	2.568	3.126	3.354
Pd	def	dφphen	2.047	2.568	3.162	3.389
Pd	dmm	dφphen	2.081	2.589	3.134	3.373
Pt	tcne	dφphen	1.669	2.158	2.895 ^b	—
Pt	fn	dφphen	1.884	2.389	3.060 ^c	3.290
Pt	dmf	dφphen	1.942	2.482	3.130 ^c	3.355 ^c
Pd	dmf	phen	2.139	2.746	—	—
Pd	dmf	bpy	2.157	2.740	—	—
Pd	dmf	4-dmbpy	2.226	2.782	—	—
Pd	dmf	5-dmbpy	2.257	2.839	—	—
Pd	dmf	tmbpy	2.341	2.926	—	—
Pd	tcne	bpy	1.845 ^b	—	—	—
Pd	ma	bpy	2.088	2.641	—	—
Pd	fn	bpy	2.115	2.661	—	—
Pd	def	bpy	2.160	2.758	—	—
Pd	dmm	bpy	2.191	2.759	—	—
Pt	dmf	bpy	2.032	2.650	—	—
Pt	dmf	tmbpy	2.217	2.836	—	—

a) ± 5 mV vs. Ag/AgNO₃(sat.). b) Cathodic peak potential. c) Scan rate 0.25 V s⁻¹.

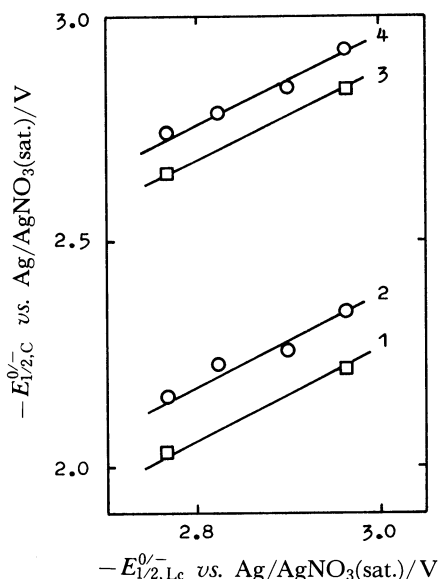


Fig. 2. $E_{1/2,C}^{0/-}$ vs. $E_{1/2,Lc}^{0/-}$ for (1) [Pt(dmf)Lc] and (2) [Pd(dmf)Lc], and $E_{1/2,C}^{0/-}$ vs. $E_{1/2,Lc}^{0/-}$ for (3) [Pt(dmf)Lc] and (4) [Pd(dmf)Lc] with Lc=bpy, 4-dmbpy, 5-dmbpy and tmbpy.

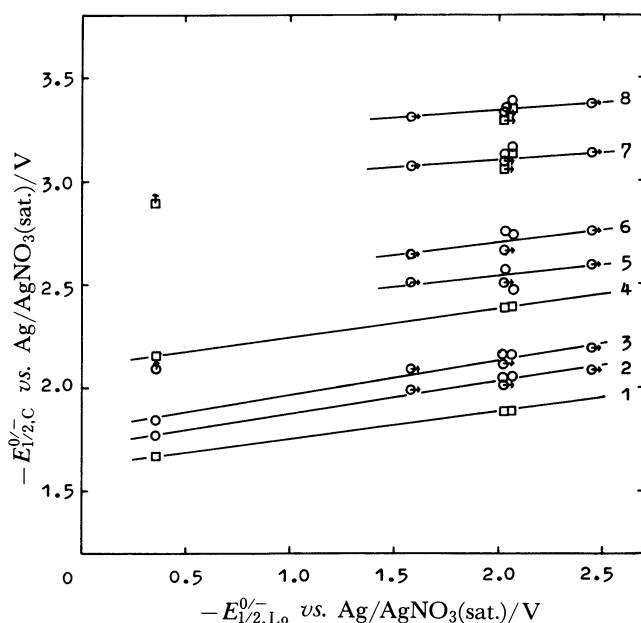


Fig. 3. $E_{1/2,C}^{0/-}$ vs. $E_{1/2,Lo}^{0/-}$ for (1) [PtLo(d ϕ phen)], (2) [PdLo(d ϕ phen)] and (3) [PdLo(bpy)], $E_{1/2,C}^{0/-}$ vs. $E_{1/2,Lo}^{0/-}$ for (4) [PtLo(d ϕ phen)], (5) [PdLo(d ϕ phen)] and (6) [PdLo(bpy)], (7) $E_{1/2,C}^{2/3-}$ vs. $E_{1/2,Lo}^{0/-}$ for (\square) [PtLo(d ϕ phen)] and (\circ) [PdLo(d ϕ phen)], and (8) $E_{1/2,C}^{3/4-}$ vs. $E_{1/2,Lo}^{0/-}$ (\square) [PtLo(d ϕ phen)] and (\circ) [PdLo(d ϕ phen)] with Lo=tcne, ma, fn, dmf, def and dmm. Experimental points with horizontal and vertical arrows are plotted with cathodic peak potentials for olefinic ligands and complexes, respectively. The arrows show the direction in which reversible half-wave potentials are located.

which was derived by assuming that the redox orbital is a ligand π^* -orbital. Figure 3 shows $E_{1/2,C}^{red}$ vs. $E_{1/2,Lo}^{0/-}$

plots for [M(0)Lo(d ϕ phen)] and [Pd(0)Lo(bpy)] with Lo=tcne, dmf, and def. The experimental points of Fig. 2 obey Eq. 1. The straight lines of Fig. 3, however, are only tentative, because experimental points for appropriate $E_{1/2,Lo}^{0/-}$ values are lacking. However, it is evident that $E_{1/2,C}^{red}$ vs. $E_{1/2,Lo}^{0/-}$ has a positive slope of 0.1–0.2, when the experimental points for the irreversible Lo $^{0/-}$ steps of ma, fn, and dmm are taken into consideration. These findings, together with features (2) and (4) of Tables 1 and 2, lead to the conclusion that the two electrons added to [M(0)LoLc] occupy the LUMO of this complex, which is dominated by a diimine ligand π^* -orbital. Unfortunately, the lack of data on reversible $E_{1/2,Lo}^{red}$ makes it difficult to assign the third and fourth steps of [M(0)Lo(d ϕ phen)] which molecular orbital an electron occupies a molecular orbital mainly of an olefinic orbital character or a diimine orbital one. However, taking into account $E_{1/2,Lo}^{0/-}$ values of ma, fn and dmm, the coordination of tri and tetra-anions of d ϕ phen can be concluded for the following reasons: First, the third and fourth steps cannot be ascribed to the reduction of coordinated Lo's because [M(0)(dmf)(bpy)] and [M(0)(dmf)(phen)] exhibit no such steps. Secondly, $E_{1/2,C}^{2/3-}$ and $E_{1/2,C}^{3/4-}$ do not depend on $E_{1/2,Lo}^{0/-}$ or the type of metal at all. This suggests that the redox orbital in these steps should be localized on the coordinated d ϕ phen molecules.

Strikingly, the excess electrons of [M(0)LoLc] occupy the Lc π^* -orbitals inspite of the fact that they are higher-lying than the Lo π^* -orbitals in a free ligand, e.g. the $E_{1/2,Lo}^{0/-}$ of tcne is by 2.4V more positive than the $E_{1/2,Lc}^{0/-}$ of bpy. One of the probable reasons may be the stabilization of the diimine π^* -orbitals caused by coordination, and the instabilization of the olefin π^* -orbitals. Although the same stabilization is seen in [M(0)(bpy) $_3$] (M=Cr and Mo),⁸ the stabilization energy is considerably greater in [M(0)LoLc] than in [M(0)(bpy) $_3$]. This may be due to the coexistence of Lo operating as an electron acceptor. This is suggested by the finding that the IR spectra of the Lo is shifted to lower frequencies upon coordination. The instabilization of the olefin π^* -orbital, on the other hand, can be ascribed to the structural change of the olefin ligand caused by coordination. Such a change is suggested by the experimental finding that the olefin C–C bond distance is longer in the complex than in the free ligand, probably due to a decrease in π -conjugation caused by the metal-to-ligand back donation.⁹ A similar π -conjugation decrease in [M(0) $_2$ (dibenzylideneacetone) $_3$] (M=Pd and Pt) was discussed in Part I.³ Also, X-ray and neutron diffraction studies of [Pt(0)-(tcne)(PPh $_3$) $_2$] show that the configuration around the ethylene carbons is essentially tetrahedral. Consequently, the ligand-metal bond is equivalent to that of the two metal-alkyl σ -bonds.¹⁰

References

- 1) N. Ito, T. Saji, and S. Aoyagui, *J. Electroanal. Chem.*, **144**, 153 (1983).
 - 2) G. M. Badger and W. H. F. Sasse, "Advances in Heterocyclic Chemistry," ed by A. R. Katritzky, Academic Press, New York (1963), Vol. 2, p. 180
 - 3) T. Ito, S. Hasegawa, Y. Takahashi, and Y. Ishii, *J. Organomet. Chem.*, **73**, 401 (1974).
 - 4) N. Ito, T. Saji, K. Suga, and S. Aoyagui, *J. Organomet. Chem.*, **229**, 43 (1982).
 - 5) M. Herberhold, "Metal π -complexes," Elsevier, Amsterdam (1972) Vol. 2, p. 263.
 - 6) T. G. Groshens, B. Henne, D. Bartak, and K. J. Klabunde, *Inorg. Chem.*, **20**, 3629 (1981).
 - 7) T. Saji and S. Aoyagui, *J. Electroanal. Chem.*, **110**, 329 (1980).
 - 8) T. Saji and S. Aoyagui, *J. Electroanal. Chem.*, **63**, 405 (1975).
 - 9) V. Graves and J. H. Lagowski, *Inorg. Chem.*, **15**, 577 (1976); D. W. Clark and K. D. Warren, *J. Organomet. Chem.*, **162**, 83 (1978); S. Evans, J. C. Green, and S. E. Jackson, *J. Chem. Soc., Faraday Trans.*, **2**, **68**, 249 (1972).
 - 10) M. L. H. Green, "Organometallic Compounds," Methuen, London (1968) Vol. 2, p. 16—18.
-